J. Chem. Sci. (2018) 130:29
https://doi.org/10.1007/s12039-018-1433-4

REGULAR ARTICLE

Temperature effects on the hydrophobic force between two graphene-like surfaces in liquid water

TUHIN SAMANTA and BIMAN BAGCHI*
Solid State and Structural Chemistry Unit, Indian Institute of Science, Bangalore, Karnataka 560 012, India
E-mail: bbagchi@sscu.iisc.ernet.in; profbiman@gmail.com

MS received 7 December 2017; revised 26 January 2018; accepted 11 February 2018; published online 2 March 2018

Abstract. Water-mediated, effective, long-range interaction between two hydrophobic surfaces immersed in water is of great importance in natural phenomena. We perform the molecular dynamics simulations to investigate the effect of temperature on the attractive force between two graphene-like hydrophobic surfaces in SPC/E water. We systematically calculate the force between two hydrophobic surfaces at different inter-wall separations (d) and subsequently determine the correlation lengths at different temperatures. A significant change in the strength of the attractive hydrophobic force is observed with the variation of temperature. The correlation length of effective hydrophobic force increases on lowering the temperature. We also examine the temperature effects on the behavior of confined water molecules by computing the density and orientational profiles. The analyses of these profiles suggest that the layering of water molecules induced by surfaces decreases with increase in temperature of the system. Critical dewetting distance (d_c), where drying transition phenomenon occurs, shifts to the lower value of d upon cooling.

Keywords. Hydrophobic force; correlation length of HFL; drying transition; tetrahedral order parameter.

1. Introduction

The interactions between hydrophobic solutes have numerous applications in several colloidal and biomolecular assemblies and in the formation of protein complexes.[1–7] One of the important manifestations of the hydrophobic interactions is observed in oil-water de-mixing because of the low solubility of hydrophobes (i.e., oil) in water.[1] Several controlled experimental studies directly measured the range and nature of interactions between the two large hydrophobic surfaces inside solutions. It was Israelachvili,[8,9] who first mentioned that the interaction force between two large hydrophobic surfaces is *attractive and long range* (*i.e.*,100–1000 Å) in nature. Recent developments in this area debated the length scales of the hydrophobic attraction. The initial outcome of 100 Å length scale was later considered to be the part of the 'short-ranged' hydrophobic interaction, while the observed 'long-ranged' force that could extend beyond 3000 Å was attributed to such artefacts as aeration.[10,11] However, Ducker and co-workers[12] reported a different observation that in the case of concentrated aqueous salt solution hydrophobic force could become insignificant beyond 50 Å. This study did not negate the possibility of longer range hydrophobic force in neat water. Recently Surface Force Apparatus (SFA) and Atomic Force Microscope (AFM) measurements established the existence of short-range force with correlation lengths of 3–7 Å.[13–15]

One of the signatures of the short ranged hydrophobic interactions is drying/dewetting transition.[16] *When two large hydrophobic surfaces immersed in water approach each other, coalescences take place between them at a particular inter-surface separation* (*i.e., known as critical distance* (d_c)). *Water is in a metastable state with respect to its vapor at that particular distance. This phenomenon is known as drying transition.* This drying/dewetting transition is essentially dependent on the thermodynamic conditions of the system and on the nature of hydrophobic surfaces. There are several theoretical and experimental studies in literature regarding the possible mechanism/origin of attractive hydrophobic force law (HFL) and about the detailed understanding (i.e., thermodynamics and kinetic pathways) of the de-wetting transition.[17–33] However, the quantitative

*For correspondence

Electronic supplementary material: The online version of this article (https://doi.org/10.1007/s12039-018-1433-4) contains supplementary material, which is available to authorized users.

understanding of such hydrophobic force remains somewhat unclear.

Theoretical understanding of hydrophobic interaction was based on a theory proposed by Pratt and Chandler, where the solute-solvent interaction was treated perturbatively.[34] Subsequently, an elegant microscopic density functional theory (DFT) was proposed by Lum *et al.,*[16] to illustrate the origin of HFL. This theory semi-quantitatively explains the attractive hydrophobic force law between two hydrophobic objects at small and large length scales.

However, a few earlier theoretical studies, using molecular dynamics simulations, have focused on the phase behavior of confined water particularly by varying the thermodynamic conditions of the systems. In an important simulation study, Parker *et al.,* studied the temperature effects on the attractive forces between two hydrophobic surfaces.[35] Their calculation revealed that there is a remarkable enhancement in the strength of attractive hydrophobic force upon heating/increasing temperature of the system. Subsequently, in another study, Berne and co-workers[22] investigated the temperature dependent associations and drying transitions of hydrophobic solutes. Their study revealed that the critical dewetting distance increases with increase in the temperature of the system. Recently, Debenedetti and co-workers[36,37] also examined the structural behavior of confined water molecules between the extended surfaces at different thermodynamic conditions. From the density profile analysis, they concluded that confined water becomes more structured upon pressurization or cooling. Importantly, they found that the effective hydrophobicity of the surfaces decreases upon pressurization or cooling of the system because of vapor phase suppression. In the recent past, considerable amount of investigations have been devoted to the hydrophobicity induced evaporation/condensation transition of the confined water through computer simulation studies which have several technological applications.[38–41]

In this work, we report the effect of temperature on the strength/range of hydrophobic force law (HFL) and on the drying/dewetting transition in terms of number density fluctuations of water confined between two graphene-like surfaces using computer simulations. The organization of the rest of the paper is as follows. In section 2, we present the simulation details. This is followed by a discussion of detailed calculations and results of the hydrophobic force law of water between two hydrophobic surfaces at different thermodynamic conditions in section 3. We construct the density profile of water molecules to describe the temperature dependent structural modification of the confined water. Additionally, in order to further analyze the water structure inside the confinement, we calculate the local tetrahedral order parameter profiles for different temperatures. We compute the isothermal compressibility of the confined water molecules to determine the effect of temperature on the critical dewetting distance. Thereafter, we briefly summarize our results in section 4.

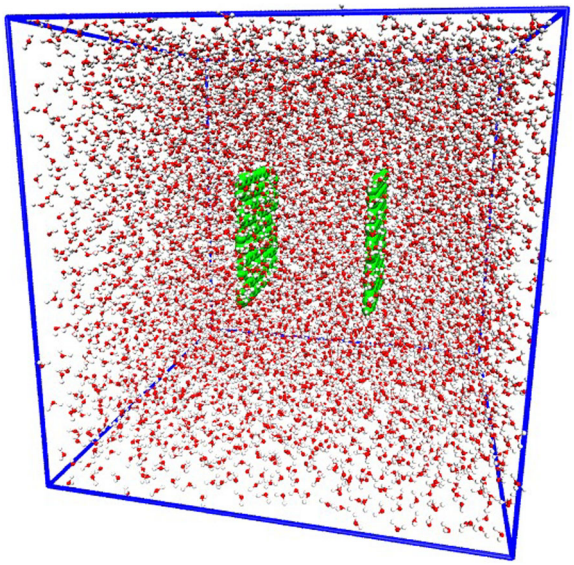

Figure 1. A representative snapshot of the simulation of the system with two hydrophobic walls immersed in liquid water. The water molecules between two hydrophobic walls are referred to as confined water and outside the hydrophobic walls are known as bulk water.

2. Simulation details

Simulations are performed using Large-scale Atomic/Molecular Massively Parallel Simulator (LAMMPS) MD packages. In this study, we use extended single point charge water (SPC/E) model.[42] We use a cubic simulation box with periodic boundary conditions applied in all three directions. We create the two hydrophobic walls (represented by a rigid, hexagonal, lattice of Lennard-Jones (LJ) atoms with a lattice constant of 1.4 Å) of dimension 19.6 × 19.4 Å^2 (for simplicity, we refer to this as 20 × 20 Å^2 surface) by mimicking the arrangements of carbon atoms in a graphene sheet. There is a gas-like density area of typically 2–3 Å width near each wall. The walls are non-interacting between each other. The two hydrophobic walls are oriented parallel to each other and also parallel to the *XY* plane (shown in Figure 1). The walls are immersed in water (i.e. with respect to the centre of the box) at the desired distance (d) by replacing certain water molecules present within contact distance. The force field parameters for wall-water interactions are taken from Ref. 29. We examine the distance dependence of the hydrophobic effects by performing a set of simulations with an inter-wall separation distance (d), ranging from 7 to 30 Å. To avoid any artefacts due to periodic boundary conditions, we use sufficiently large box size. The number of water molecules varies in our simulations depending on the inter-wall separations. For example,

in case of small inter-wall separation ($d = 7 - 20$ Å), we use 7200 water molecules (box size ~ 60 Å × 60 Å × 60 Å), whereas for large ($d = 25$–30 Å) inter-wall separation ~ 9500 water molecules (box size ~ 67 Å × 67 Å × 67 Å) are required to fully solvate the box.

We perform the MD simulations in the isothermal-isobaric ensemble (NPT) at 1 bar pressure and at various constant temperatures (T = 240 K, 270 K, 300 K, 330 K and 360 K), by using the Nosé -Hoover[43,44] barostat and thermostat. The system is then equilibrated for 10^5 steps at constant temperature and volume, with each time step $\tau = 2$ fs. The production run is carried out for 10^7 steps at constant temperature and volume.

The particle–particle particle–Mesh (PPPM) Ewald method is used to compute long-range corrections of electrostatic interactions. The k-space is taken to be 0.0001 $Å^{-1}$, and calculations are performed on a 15 × 15 × 15 grid, with rms precision of 4×10^{-5}, which are the standard PPPM Ewald parameters in LAMMPS. We use a 10Å cut-off value for the Lennard–Jones interactions.

3. Results and Discussion

3.1 *Calculation of effective hydrophobic force between the walls*

To explore the effects of hydrophobic walls on each other, we calculate the resultant force between the two walls in the following manner. First, we consider the water molecules which are confined between the two hydrophobic walls and also outside the walls. We project the forces obtained from these water molecules along the inter-wall separation axis i.e., Z-axis. The force between the two walls is finally obtained as $F_{cav}(d) = F_L - F_R$, where F_L and F_R are forced on the left and the right walls respectively. It is worth mentioning here, that each wall experience forces exerted by both the confined water molecules from inside and bulk water molecules from outside. To obtain the force, first, we have to calculate the pressure on each wall. Now, pressure on the walls[45–47] can be calculated from the well-known virial equation,

$$P_w = \frac{Nk_BT}{V} + \frac{\sum_i r_i f_i}{DV} \tag{1}$$

where N is the number of atoms in the system, k_B is the Boltzmann constant, T is the temperature, D (= 3) is the dimensionality of the system, r_i is the position vector of the i^{th} particle and f_i is the total internal force on the i^{th} particle. In Eq. 1, the second term is the virial, arising from the intermolecular interactions. To obtain the pressure on each wall, we use the following definition, $P_w = P_{wO} + P_{wI}$, where w is L for left wall and R for right wall, P_{wO} is the pressure perpendicular to the w^{th} wall from outside and P_{wI} is the same from inside. Then we multiply the pressure on each wall by the respective surface areas to get the force exerted on the walls. Finally, the effective force (F) between the walls is obtained as, $F = F_{cav}(d) - F_\infty$, where F_∞ is the force at infinite separation between the two walls and obtained by fitting the distance dependent F_{cav}.

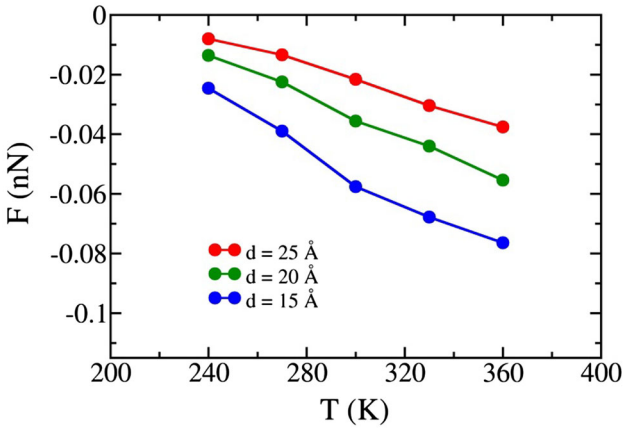

Figure 2. Effective hydrophobic force as a function of temperature. The effective force decreases with the increase of temperature.

Figure 2 shows the effective hydrophobic force between two hydrophobic walls as a function of temperature of the system, for three fixed inter-wall separations (d). We find that the magnitude of effective hydrophobic force between two surfaces increases with the increase in temperature of the system. For all the studied temperatures, the effective force between two hydrophobic surfaces decreases as the inter-wall separation between the two hydrophobic walls increases.

The negative force indicates an effective attraction between the walls, induced by the intervening water molecules. As shown in Figure 3, the attractive force between the hydrophobic walls increases bi-exponentially with decrease of d. Several scientists, notably Israelachvilli *et al.,*[8,10] observed such strong attractions between the hydrophobic surfaces. We find that the range of effective hydrophobic force increases with decrease in temperature of the system (Table 1).

This effective force can be fitted by the following equation

$$F = a_{F_1} \exp(-d/\xi_{F_1}) + a_{F_2} \exp(-d/\xi_{F_2}). \tag{2}$$

where d is the inter-wall distance, $a_{F_1}, a_{F_2}, \xi_{F_1}$ and ξ_{F_2} are fitting parameters. The fitting parameters are provided in Table 1.

In the long-range limit (in the context of the present simulations), the prediction of correlation length is in good agreement with the experiments of Israelachvili *et*

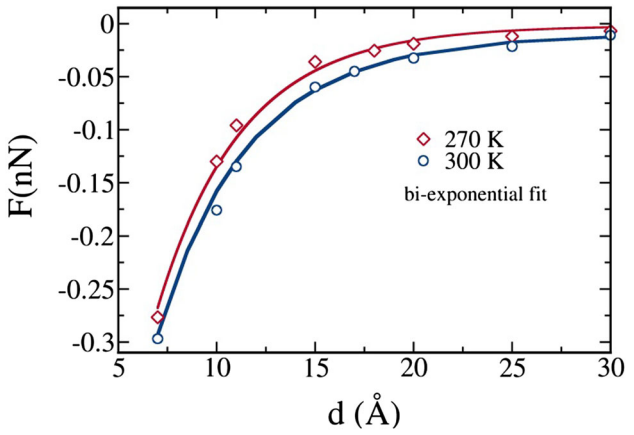

Figure 3. Effective hydrophobic force (F) as a function of inter-wall separation. The solid blue line is the bi-exponential fit with correlation lengths of 4.92 and 19.40 for 300 K. Solid maroon line is the bi-exponential fit with correlation lengths of 4.34 and 23.1 for 270 K.

Table 1. Fitting parameters of the hydrophobic force law (HFL) (see Eq. 2) for two different temperatures (T = 300 K and 270 K). Fitted values of correlation length and correlation coefficient (R-square) for two different temperatures are shown here.

Temp (T)	a_{F_1}	a_{F_2}	ξ_{F_1}	ξ_{F_2}	R-square
300 K	−1.39	−0.041	4.92	19.40	0.992
270 K	−1.35	−0.008	4.34	23.10	0.997

al.[8] This is also consistent with the experimental findings of Pashley and co-workers,[48] where they have found that the attractive forces between planar, uncharged hydrophobic surfaces (in water solution) have a correlation length of about 15 Å.

The semi-log plot of attractive force shown in Figure 4 clearly depicts the two distinctly different regions and shows a crossover[49] between the two regimes. This resembles the de-wetting/drying phenomenon which was predicted by earlier theoretical studies.[16,20,22,23] When the water-surface interactions fail to reasonably account for the lost water-water interactions at an interface then there is a free energy drive for phase separation and interfacial collapse.

As shown in Figure 4, the semi-log plot of effective force shows a sharp crossover near 12–14 Å inter-wall separations for 300 K, whereas, for 270 K this crossover is noticed around 11 Å of inter-wall separation. We find that the sharp crossover between the two regions shifts to lower value of d upon cooling. Similar to several recent experimental findings,[13–15] we also find that one more crossover is possible near 5 Å (not shown here) of separations between two hydrophobic walls where hardly

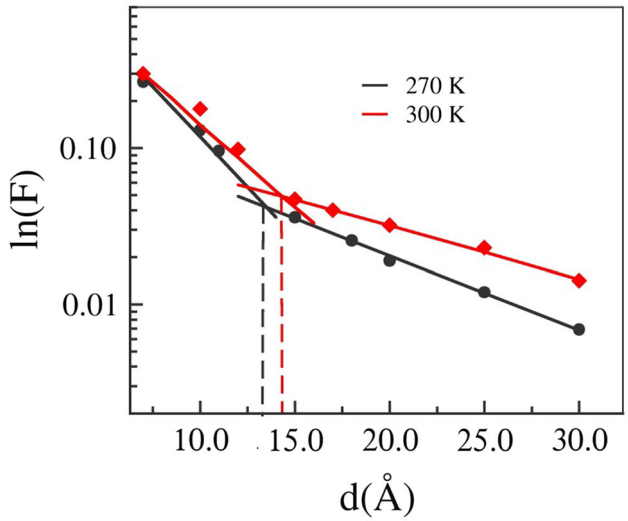

Figure 4. Semi-log plot of effective hydrophobic force (F) is plotted against the inter-wall separation (d), for T = 270 K and T = 300 K. The figure depicts a clear crossover between the two regimes for both the temperatures.

any volume (except single file) of water molecules exist. This is expected on physical grounds as water molecules may be forced out by direct attraction between two walls.

From this study, we observe the reduction of effective hydrophobicity of plates upon cooling. This is mainly because of the fact that lowering of temperature increases the effective attraction of the water molecules towards hydrophobic surfaces and subsequently the effective hydrophobicity of the wall reduces. This phenomenon was also reported in the previous studies.[35,37,50,51]

3.2 *Density profile*

In order to understand the attractive force between two hydrophobic surfaces, several prior theoretical studies focused on the density-dependent theories.[16,34] In our study we also investigate the structural behavior of the confined water molecules. To study the effect of temperature on the water structure we calculate the water density profile at different inter-wall separations (Figure 5). Water molecules within the cavity are in dynamical equilibrium with the outside bulk molecules. Finally, the density of water molecules confined between two hydrophobic walls[31] is calculated using the standard formula given by,

$$\rho_{cav} = \frac{\overline{N_{cav}}}{V_{cav}} \tag{3}$$

where confined volume is defined as, $V_{cav} = dA$ and A is the area of the surface. $\overline{N}$ is the average number of water molecules present in the volume V_{cav}.

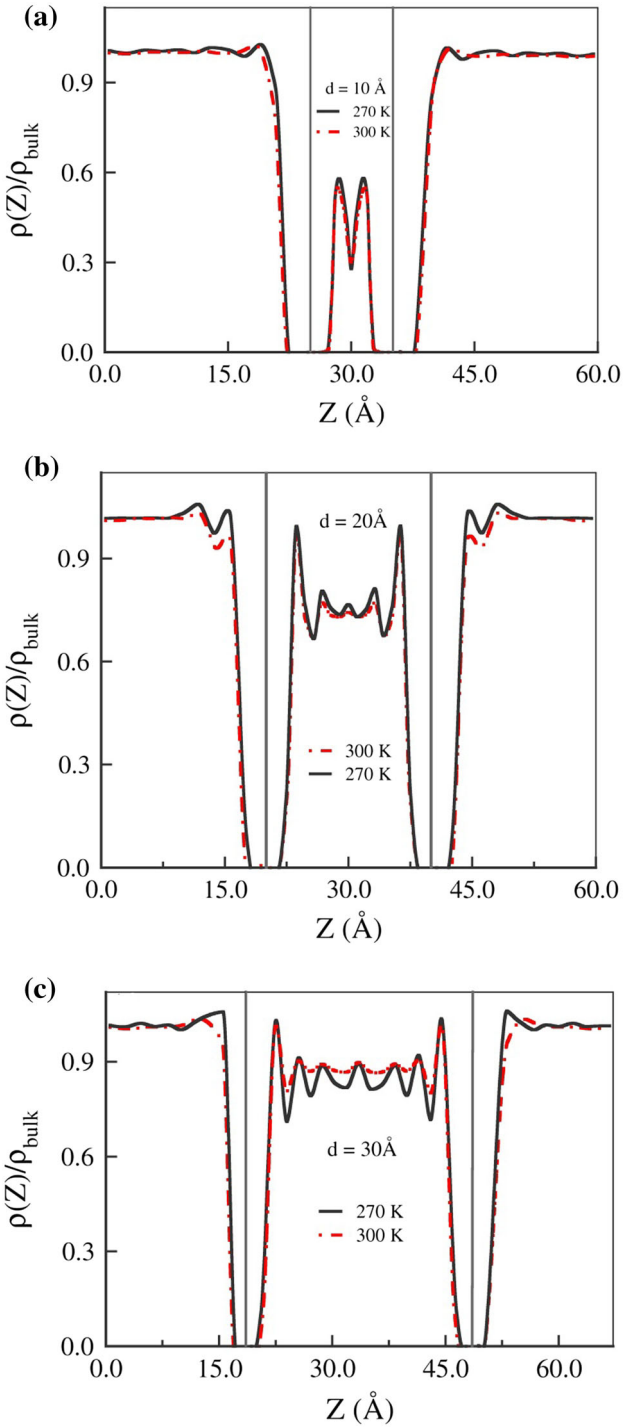

Figure 5. Local normalized density profile ($\rho(Z)/\rho_{bulk}$) of water for different inter-wall separations d, (a) $d = 10$ Å, (b) $d = 20$ Å and (c) $d = 30$ Å for T = 270 K and T = 300 K. The thick grey lines are the schematic representation of the two hydrophobic walls.

In this calculation, we define the distance (Z) dependent density, $\rho(Z)$, by following a coarse-graining where we divide the whole cavity region into small boxes. The region confined between two hydrophobic plates is sub-divided into several small grids and the center of each grid represents the distance from the left wall (Z). We use a similar coarse-grain procedure to calculate the distance (Z) dependent density for the outside regions of the hydrophobic walls. Symmetric nature of the confinement suggests that two grids located at the same distance from the respective walls should have the same local density. We therefore improve statistics by averaging over the small boxes at the same Z value.

As shown in Figure 5, the maxima of $\rho(Z)$ become sharper upon cooling indicating the enhancement of water structure. The multiple layered structures formed by water molecules between the two hydrophobic walls are manifested in the oscillations of density profile along Z-direction. The surface-induced layering of water molecules inside the confinement increases on lowering the temperature of the system. Figure 5(c) shows the pronounced effect of lowering temperature at large inter-wall separation. For all the different temperatures studied, at large inter-wall separation, the confined water density approaches that of the bulk value. We further observe with the decrease in temperature of the system, the peak of $\rho(Z)$ closest to each hydrophobic wall exhibits slight asymmetrical broadening toward the hydrophobic plates.

From the density profile analyses, we observe that both the number and layering of water molecules between the hydrophobic walls increase with a decrease in temperature of the system. These observations indicate that, as we reduce the temperature of the system, the hydrophobic surfaces become more attractive towards water molecules and consequently the effective hydrophobicity of hydrophobic walls decreases.

It is clearly seen from Figure 5 that the structure of water molecules in the confined region is different from that outside. This is because of the confinement-induced ordering that is partly absent outside the hydrophobic surfaces. Hydrophobic force law (HFL) arises due to the interaction between the density inhomogeneity created by the two surfaces (gas-like density near each surface) that propagates inward from the surfaces.

Figure 6 shows that for three fixed inter-wall separation of hydrophobic walls, the normalized cavity density of water molecules increases upon cooling. It was already reported in the literature that the confined water density increases substantially with a decrease in temperature for hydrophobic confinement as opposed to hydrophilic confinement.[37]

In the simulation, water molecules remain in the liquid phase in the region outside the confinement of the hydrophobic walls, for all the studied temperatures (i.e., from 240 K to 360 K). In Figures S1 and S3, we show some representative snapshots of the simulations

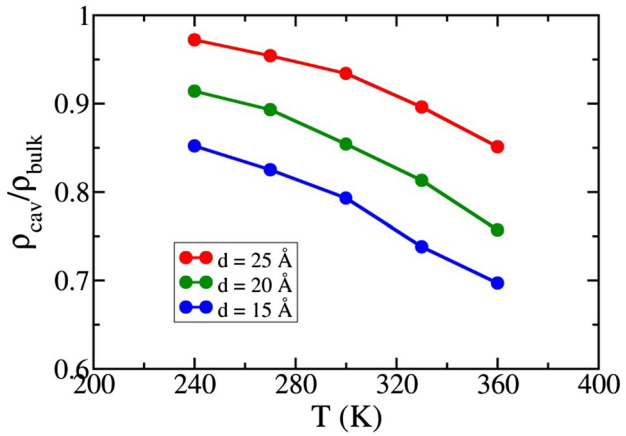

Figure 6. Average normalized cavity density of confined water molecules as a function of temperature. The confined water density gradually increases with a decrease in the temperature, for all the fixed inter-wall separations.

at low temperatures. The random ordering of the water molecules (i.e., the absence of any ordered hexagonal ice-like rings) in the confined water establishes the liquid state of water at low temperatures. It is to be noted that phase diagram of SPC/E water shows the existence of liquid water from 240 K to 360 K temperature range.[52,53]

3.3 *Orientational profile*

The density of water is partly slaved to the orientation of the water molecules (by H-bond network). Thus, we analyze the confined structure of water molecules between two large hydrophobic surfaces by calculating the orientational order parameter. In order to understand the relative orientation of water molecules within the hydrophobic confinement, we consider a different (but well-known) order parameter, namely the local tetrahedral order parameter which is described as[54]:

$$t_h = 1 - \frac{3}{8}\sum_{j=1}^{3}\sum_{k=j+1}^{4}\left(\cos\psi_{jk} + \frac{1}{3}\right)^2. \qquad (4)$$

For perfect tetrahedral arrangement t_{he} reaches its maximum value unity and for a non-interacting system, the average value of t_h is zero. This parameter can be employed to analyze the local structure or packing. Similar to the calculations of density profile we calculate the tetrahedral order parameter profile in coarse-graining method.

In Figure 7, we plot the average local tetrahedral order parameter of the confined water molecules in each grid as a function of Z.

In case of large inter-wall separation (d), the local tetrahedral order parameter value increases and local water structure becomes bulk-like in the center of the

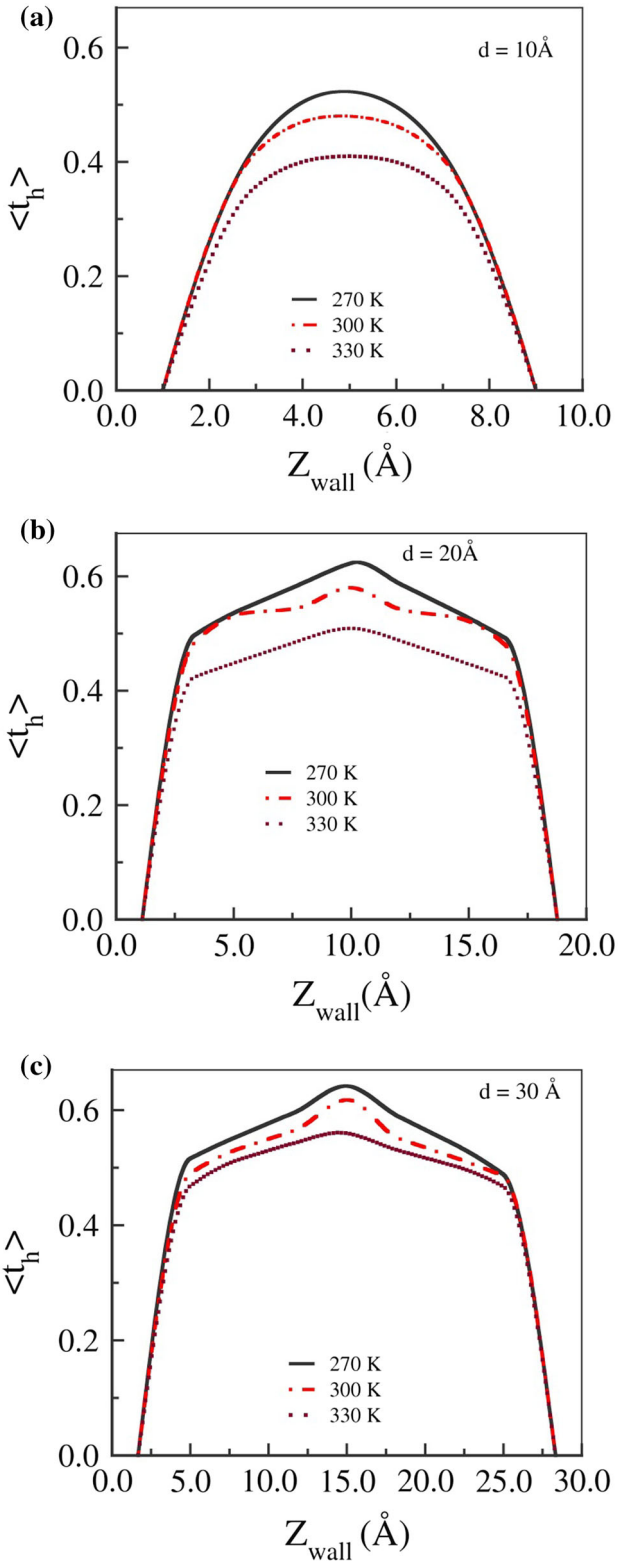

Figure 7. The average tetrahedral order parameter value within a grid (i.e., rectangular box) along the axis of separation of the distance between two hydrophobic walls, at different inter-wall separations d, (a) d = 10 Å, (b) d = 20 Å and (c) d = 30 Å, for temperatures T = 270 K, T = 300 K and T = 330 K. The bulk values of tetrahedral order parameter for different temperatures are, t_h = 0.71 (at 270 K); t_h = 0.64 (at 300 K); and t_h = 0.55 (at 330 K).

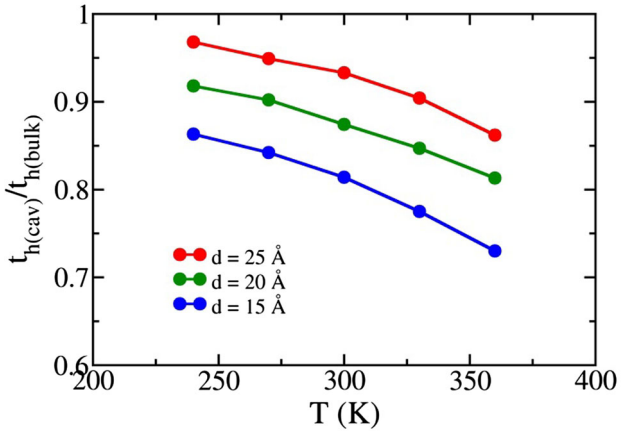

Figure 8. Average normalized tetrahedral order parameter value of confined water as a function of temperature. This figure indeed illustrates the enhancement of the local structure of confined water molecules upon cooling. The local tetrahedral order parameter value is normalized with respect to the bulk value.

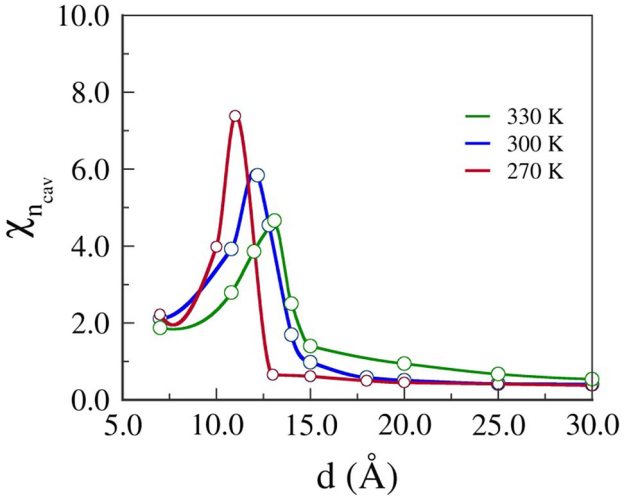

Figure 9. Local compressibility of confined water calculated from number density fluctuations in the water confined within the three-dimensional box formed by the two walls, for T = 270 K, T = 300 K and T = 330 K. The local compressibility is plotted against the distance of separation *d* between the two plates.

confined region for all the studied temperatures (Figure 7(c)). The average local tetrahedral order parameter value increases in regions progressively closer to the plates with a decrease in temperature of the system. For all the studied temperatures, the number of H-bonds in the middle of the confined region almost approaches the bulk value that results in the increase in the value of local tetrahedral order parameter. The low value of average local tetrahedral order parameter nearby the walls is because of the fact that the number of H-bonds among the water molecules is reduced by the presence of the walls.

Similar to that of density, orientational profiles also indicate the enhancement of local structure of cavity water molecules with a decrease in temperature of the system. As shown in Figure 8, for fixed interwall separations, the enhancement of tetrahedral order parameter essentially suggests the extent of formation of the more ordered tetrahedral structure of confined water molecules upon cooling. This is because of the fact that increases in temperature of the system causes a decrease in the number of H-bonds of the water molecules inside the confinement. The orientaional heterogeneity across the walls is the origin for the long-range hydrophobic interactions between the hydrophobic surfaces.[45,49]

The liquid phase of water molecules at low temperatures (i.e., 240 K and 270 K) is further verified by calculating the Steinhardt bond order (local) parameter (Q_6)[55] for water molecules of interest. The distributions of the local order parameters and their average values suggest that water remains in the liquid phase at low temperatures (Figures S2 and S4 in Supplementary Information).

3.4 *Local isothermal compressibility*

In our study, as discussed above, two walls are immersed within the water. There exists an area that represents gas-like density near each surface, which is typically 2–3 Å wide. The decrease in the number of H-bonds near the extended hydrophobic surfaces causes the water to move away from the surfaces, producing a thin vapor-like layer. This causes fluctuations at the interfaces and expels the remaining liquid between these surfaces (when they are sufficiently close to each other).

In order to explore the crossover observed in the attractive hydrophobic force, we compute one of the important response functions, isothermal compressibility. From this response function, we can precisely investigate the effect of temperature on such crossover. Local compressibility is defined as,

$$\chi_{n_{cav}} = \frac{\langle n_{cav}^2 \rangle - \langle n_{cav} \rangle^2}{\langle n_{cav} \rangle} \tag{5}$$

where n_{cav} is the number of water molecules inside the cavity of volume V in between the two hydrophobic walls.

The local compressibility of the confined water molecules goes through a maximum (Figure 9), which suggests the crossover from a gas like a region to a liquid like a region. The divergent like behavior in the local compressibility indicates that system passes through a free energy minimum.

In Figure 9, we observe that the drying transition occurs near $d \sim$ 13–14 Å for 330 K temperature, $d \sim$

12 Å for 300 K temperature, and $d \sim 11$ Å for 270 K temperature. We find that the critical inter-wall separation (d_c) changes to lower value of d upon cooling. This observation is in good agreement with the earlier studies by Berne and co-workers.[18,50] The estimate of critical de-wetting distance at 300 K is also consistent with the study of Zhou *et al.*[56] They found that the critical de-wetting transition between two hydrophobic surfaces takes place at d $\sim$ 12 Å, in pure water.

At 300 K temperature, the number of confined water molecules, $n_{cav}^{(water)}$ starts increasing slowly with the increase in the inter-wall separation (d), from 7 Å onwards, and it jumps to a large value (approximately 85) at $d = 12$ Å, then again it continues to increase gradually upto 30 Å. The small number of water molecules at $d < 12$ Å indicates that a vapor phase is dominant between the two hydrophobic walls (i.e., confined water molecules are unstable in its liquid state) (shown in Figure S5). On the other hand, at $d \geq 12$ Å water molecules form a liquid phase in the confinement. A similar phenomenon is also observed for other temperatures corresponding to their critical de-wetting distances. We find that at an inter-wall separation $d < 7$ Å ($\sim$ 5 Å), complete drying is observed with hardly any volume of water molecules between the walls.

4. Conclusions

The hydrophobic interaction plays a crucial role in protein and micellar aggregation, lipid bilayer formation and other biological self-organizing processes.[57,58] Hydrophobic force arises because of long-range interactions between the hydrophobic surfaces. While, the initial landmark experiments by Israelachvili *et al.*,[8,9] indicated a rather long ranged attractive hydrophobic force, later experiments seem to propose a somewhat shorter ranged force. Clearly, the range of the force shall depend strongly on the nature of the roughness of the surfaces, and also on the thermodynamic conditions of the system.

In this work, we present the direct calculation of the strength/range of attractive hydrophobic force and phase behavior of water molecules confined (i.e., liquid) between two hydrophobic walls at different thermodynamic conditions. As shown in Figures 2, 3 and 4, we find that there is a significant change in the magnitude of the effective attractive force between two hydrophobic surfaces and in a correlation length of HFL upon cooling. The correlation length/range of effective hydrophobic force increases on lowering the temperature. The effective hydrophobic force exhibits bi-exponential distance dependence that shows two length scales of hydrophobicity. While the smaller correlation length at small separation d can be understood easily in terms of the gas-like state of the system at those values of d, the larger correlation of 20 Å at larger d can be regarded as a persistence length of density fluctuations. A sharp crossover between the two regimes in the distance dependence of attractive force (Figure 4) is further reflected in the divergent-like growth of the local isothermal compressibility of the confined water molecules (Figure 9). The crossover from shorter range to longer-range force is rather sharp, reminding one of a 'drying/dewetting transition'. This study reveals that the critical dewetting distance, which was predicted by several earlier theoretical studies,[16,23,34] decreases to lower value of d with a decrease in temperature (Figures 4 and 9).

The present work demonstrates that there is a weakening of the effective hydrophobicity of the surfaces upon cooling. This phenomenon has important consequences on the thermodynamic/structural properties of the confined water. From the density calculations, we find that the structure of water molecules in the confined region is dissimilar from that of outside region (Figure 5). Both the water density and layering of water molecules inside the confinement increase on lowering the temperature of the system (Figures 5 and 6). Furthermore, the present study brings out the role of molecular orientation (tetrahedral order parameter of confined water molecules) in defining the HFL. The increase in the local tetrahedral order parameter value upon cooling signifies the enhancement of microscopic structure (i.e., tetrahedral arrangements) of water molecules in confinement (as shown in Figures 7 and 8). Finally, we conclude this by noting that hydrophobic walls become *more attractive toward the water molecules upon cooling*.

Supplementary Information (SI)

Figures S1-S5 are available as Supplementary Information at www.ias.ac.in/chemsci.

Acknowledgements

It is a pleasure to thank Dr. Sarmistha Sarkar, Mr. Rajesh Dutta, Mr. Saumyak Mukherjee and Mr. Sayantan Mondal for going through the manuscript. We thank DST (India) for partial support of this work. BB thanks J.C. Bose Fellowship for financial support. TS acknowledges CSIR-UGC for providing Senior Research Fellowship (SRF).

References

1. Tanford C 1973 *The Hydrophobic Effect* (New York: Wiley)

2. Kauzmann W 1959 Some factors in the interpretation of protein denaturation *Adv. Protein Chem.* **14** 1
3. Bagchi B 2013 *Water in Biological and Chemical Processes: From Structure and Dynamics to Function* (Cambridge: Cambridge University Press)
4. Ben-Naim A 1980 *Hydrophobic Interaction among Many Solute Particles. In Hydrophobic Interactions* (Boston MA: Springer) p.117
5. Dill K A, Privalov P L, Gill S J and Murphy K P 1990 The meaning of hydrophobicity *Science* **250** 297
6. Chandler D 2005 Interfaces and the driving force of hydrophobic assembly *Nature* **437** 640
7. Hummer G, Rasaiah J C and Noworyta J P 2001 Water conduction through the hydrophobic channel of a carbon nanotube *Nature* **414** 188
8. Israelachvili J and Pashley R 1982 The hydrophobic interaction is long range, decaying exponentially with distance *Nature* **300** 341
9. Israelachvili J N and Adams G E 1978 Measurement of forces between two mica surfaces in aqueous electrolyte solutions in the range 0–100 nm *J. Chem. Soc. Faraday T. 1* **74** 975
10. Meyer E E, Rosenberg K J and Israelachvili J 2006 Recent progress in understanding hydrophobic interactions *Proc. Natl. Acad. Sci. U. S. A.* **103** 15739
11. Hammer M U, Anderson T H, Chaimovich A, Shell M S and Israelachvili J 2010 The search for the hydrophobic force law *Faraday Discuss* **146** 299
12. Mastropietro D J and Ducker W A 2012 Forces between Hydrophobic Solids in Concentrated Aqueous Salt Solution *Phys. Rev. Lett.* **108** 106101
13. Tabor R F, Grieser F, Dagastine R R and Chan D Y 2014 The hydrophobic force: measurements and methods *Phys. Chem. Chem. Phys.* **16** 18065
14. Tabor R F, Wu C, Grieser F, Dagastine R R and Chan D Y 2013 Measurement of the hydrophobic force in a soft matter system *J. Phys. Chem. Lett.* **4** 3872
15. Kaggwa G B, Nalam P C, Kilpatrick J I, Spencer N D and Jarvis S P 2012 Impact of hydrophilic/hydrophobic surface chemistry on hydration forces in the absence of confinement *Langmuir* **28** 6589
16. Lum K, Chandler D and Weeks J D 1999 Hydrophobicity at small and large length scales *J. Phys. Chem. B* **103** 4570
17. Bratko D, Curtis R, Blanch H and Prausnitz J 2001 Interaction between hydrophobic surfaces with metastable intervening liquid *J. Chem. Phys.* **115** 3873
18. Hua L, Zangi R and Berne B 2009 Hydrophobic interactions and dewetting between plates with hydrophobic and hydrophilic domains *J. Phys. Chem. C* **113** 5244
19. Hua L, Huang X, Liu P, Zhou R and Berne B J 2007 Nanoscale dewetting transition in protein complex folding *J. Phys. Chem. B* **111** 9069
20. Liu P, Huang X, Zhou R and Berne B J 2005 Observation of a dewetting transition in the collapse of the melittin tetramer *Nature* **437** 159
21. Zangi R, Zhou R and Berne B 2009 Urea's action on hydrophobic interactions *J. Am. Chem. Soc.* **131** 1535
22. Berne B J, Weeks J D and Zhou R 2009 Dewetting and hydrophobic interaction in physical and biological systems *Annu. Rev. Phys. Chem.* **60** 85
23. Huang X, Margulis C J and Berne B J 2003 Dewetting-induced collapse of hydrophobic particles *Proc. Natl. Acad. Sci. U.S.A.* **100** 11953
24. Choudhury N and Pettitt B M 2007 The dewetting transition and the hydrophobic effect *J. Am. Chem. Soc.* **129** 4847
25. Remsing R C, Xi E, Vembanur S, Sharma S, Debenedetti P G, Garde S and Patel A J 2015 Pathways to dewetting in hydrophobic confinement *Proc. Natl. Acad. Sci. U.S.A.* **112** 8181
26. Giovambattista N, Debenedetti P G and Rossky P J 2007 Hydration behavior under confinement by nanoscale surfaces with patterned hydrophobicity and hydrophilicity *J. Phys. Chem. C* **111** 1323
27. Giovambattista N, Lopez C F, Rossky P J and Debenedetti P G 2008 Hydrophobicity of protein surfaces: Separating geometry from chemistry *Proc. Natl. Acad. Sci. U.S.A.* **105** 2274
28. Ferguson A L, Giovambattista N, Rossky P J, Panagiotopoulos A Z and Debenedetti P G 2012 A computational investigation of the phase behavior and capillary sublimation of water confined between nanoscale hydrophobic plates *J. Chem. Phys.* **137** 144501
29. Sharma S and Debenedetti P G 2012 Evaporation rate of water in hydrophobic confinement *Proc. Natl. Acad. Sci. U.S.A.* **109** 4365
30. Leung K, Luzar A and Bratko D 2003 Dynamics of capillary drying in water *Phys. Rev. Lett.* **90** 065502
31. Choudhury N and Pettitt B M 2005 On the mechanism of hydrophobic association of nanoscopic solutes *J. Am. Chem. Soc.* **127** 3556
32. Yethiraj A 1999 Forces between surfaces immersed in polyelectrolyte solutions *J. Chem. Phys.* **111** 1797
33. Despa F and Berry R S 2007 The origin of long-range attraction between hydrophobes in water *Biophys. J.* **92** 373
34. Pratt L R and Chandler D 1977 Theory of the hydrophobic effect *J. Chem. Phys.* **67** 3683
35. Parker J L, Claesson P M and Attard P 1994 Bubbles, cavities, and the long-ranged attraction between hydrophobic surfaces *J. Phys. Chem.* **98** 8468
36. Giovambattista N, Rossky P J and Debenedetti P G 2006 Effect of pressure on the phase behavior and structure of water confined between nanoscale hydrophobic and hydrophilic plates *Phys. Rev. E* **73** 041604
37. Giovambattista N, Rossky P J and Debenedetti P G 2009 Effect of temperature on the structure and phase behavior of water confined by hydrophobic, hydrophilic, and heterogeneous surfaces *J. Phys. Chem. B* **113** 13723
38. Brovchenko I and Oleinikova A 2010 Condensation/Evaporation Transition of Water in Spherical Pores in Equilibrium with Saturated Bulk Water *J. Phys. Chem. B* **114** 16494
39. Brovchenko I and Oleinikova A 2011 Effect of pore size on the condensation/evaporation transition of confined water in equilibrium with saturated bulk water *J. Phys. Chem. B* **115** 9990
40. Brovchenko I, Oleinikova A and Geiger A In *Water condensation in pores for heat storage: theoretical limits and prerspectives*, Proceedings of the 23rd European Symposium on Applied Thermodynamics, 2008

41. Banerjee S, Ghosh R and Bagchi B 2012 Structural Transformations, Composition Anomalies and a Dramatic Collapse of Linear Polymer Chains in Dilute Ethanol–Water Mixtures *J. Phys. Chem. B* **116** 3713
42. Berendsen H J C, Grigera J R and Straatsma T P 1987 The missing term in effective pair potentials *J. Phys. Chem.* **91** 6269
43. Nosé S 1984 A unified formulation of the constant temperature molecular dynamics methods *J. Chem. Phys.* **81** 511
44. Hoover W G 1985 Canonical dynamics: Equilibrium phase-space distributions *Phys. Rev. A* **31** 1695
45. Banerjee S, Singh R S and Bagchi B 2015 Orientational order as the origin of the long-range hydrophobic effect *J. Chem. Phys.* **142** 134505-1
46. Delville A 1993 Structure and properties of confined liquids: a molecular model of the clay-water interface *J. Phys. Chem.* **97** 9703
47. van Buuren A R, Marrink S J and Berendsen H J 1993 A molecular dynamics study of the decane/water interface *J. Phys. Chem.* **97** 9206
48. Pashley R M, McGuiggan P M, Ninham B W and Evans D F 1985 Attractive forces between uncharged hydrophobic surfaces: direct measurements in aqueous solution *Science* **229** 1088
49. Samanta T, Banerjee S and Bagchi B 2016 Crossover behavior in the distance dependence of hydrophobic force law arXiv preprint arXiv:1608.04107
50. Zangi R and Berne B 2008 Temperature dependence of dimerization and dewetting of large-scale hydrophobes: a molecular dynamics study *J. Phys. Chem. B* **112** 8634
51. Huang D M and Chandler D 2000 Temperature and length scale dependence of hydrophobic effects and their possible implications for protein folding *Proc. Natl. Acad. Sci. U.S.A.* **97** 8324
52. Vega C, Sanz E and Abascal J 2005 The melting temperature of the most common models of water *J. Chem. Phys.* **122** 114507
53. Aragones J and Vega C 2009 Plastic crystal phases of simple water models *J. Chem. Phys.* **130** 244504
54. Chau P L and Hardwick A J 1998 A new order parameter for tetrahedral configurations *Mol. Phys.* **93** 511
55. Steinhardt P J, Nelson D R and Ronchetti M 1983 Bond-orientational order in liquids and glasses *Phys. Rev. B* **28** 784
56. Ren X, Wang C, Zhou B, Fang H, Hu J and Zhou R 2013 Ethanol promotes dewetting transition at low concentrations *Soft Matter* **9** 4655
57. Bryngelson J D and Wolynes P G 1989 Intermediates and barrier crossing in a random energy model (with applications to protein folding) *J. Phys. Chem.* **93** 6902
58. Dill K A and Chan H S 1997 From Levinthal to pathways to funnels *Nat. Struct. Biol.* **4** 10